Interfacial Effects Produced by Crystallization of Polypropylene with Polypropylene-*g*-Maleic Anhydride Compatibilizers

J. DUVALL,[1] C. SELLITTI,[1] C. MYERS,[2] A. HILTNER,[1,*] and E. BAER[1]

[1]Department of Macromolecular Science and Center for Applied Polymer Science, Case Western Reserve University, Cleveland, Ohio 44106; [2]Amoco Chemical Company, Research and Development, Naperville, Illinois 60566

SYNOPSIS

Two anhydride-grafted isotactic polypropylene (PP) compatibilizers, HAC or high-anhydride compatibilizer (2.7 wt % grafted maleic anhydride) and LAC or low-anhydride compatibilizer (0.2 wt % anhydride), were compared in PP-rich blends with polyamide-66 (25 wt %). A previous article demonstrated that LAC imparted a much higher fracture strain than did HAC at similar anhydride concentrations. The present study shows that LAC is capable of cocrystallization with PP. HAC does not cocrystallize, but crystallizes as a second phase in binary PP/HAC blends studied by DSC and hot-stage microscopy. A cocrystallization model is proposed to explain the higher fracture strain of PP/LAC/PA blends. A separate phase crystallization model is proposed for PP/HAC/PA blends. The models are supported by peel tests, which demonstrate greater adhesion of PP with LAC than with HAC. © 1994 John Wiley & Sons, Inc.

INTRODUCTION

Polypropylene-grafted-maleic anhydride (PP-*g*-MA) has been shown to be an effective compatibilizer for polypropylene/polyamide blends.[1-5] The present study focuses on two PP-*g*-MA compatibilizers with different amounts of grafted anhydride and different molecular weights. Detailed analysis of the low-anhydride compatibilizer (LAC) and the high-anhydride compatibilizer (HAC) used in this work is given in the preceding article[5] along with their effect on morphology, mechanical properties, and microdeformation processes of polypropylene (PP)-rich blends with polyamide-66 (PA) (25 wt %). It was found that particle size correlated with the anhydride concentration in the blend rather than with the amount of compatibilizer used. The mechanical properties, however, were strongly dependent on the type of compatibilizer as well as on the anhydride concentration. With similar anhydride concentrations, blends compatibilized with LAC exhibited much higher fracture strains than did those with HAC. Since the particle size was similar and the number of chemical linkages between compatibilizer and PA was also presumed to be similar, this observation suggested that physical interactions between the compatibilizer and PP matrix material influenced the fracture strain. Therefore, the goal of this article was to explain the mechanical behavior of the blends by examining the physical interactions between PP and the PP-*g*-MA compatibilizers used in the blend study.

EXPERIMENTAL

Materials

Polypropylene (PP), polyamide-66 (PA), polypropylene-grafted maleic anhydride compatibilizers, and blends were supplied by the Amoco Chemical Co. The polyamide was DuPont Zytel 101, which was dried in a −30°C dewpoint oven for 12–16 h at 71°C before compounding. The PP was stabilized Amoco isotactic homopolymer with a melt-flow rate of 3.5 g/10 min. The low-anhydride compatibilizer (LAC) had an average of one anhydride group per

* To whom correspondence should be addressed.

Journal of Applied Polymer Science, Vol. 52, 207–216 (1994)
 CCC 0021-8995/94/020207-10

chain (0.2% anhydride by weight) and the high-anhydride compatibilizer (HAC) had an average of six anhydride groups per chain (2.7% anhydride by weight). Whereas the LAC had much less grafted anhydride, it also had a molecular weight approximately three times higher than that of the HAC. Detailed analysis of the compatibilizers and information on blend preparation and compositions are given in the preceding article.[5]

Methods

Samples weighing between 7 and 15 mg taken from injection-molded disks were scanned in a Perkin-Elmer DSC7 from 25 to 190°C under a nitrogen environment using a heating/cooling rate of 10°C/min. Data were collected during the first heating and cooling cycles and the second heating cycle. Isothermally crystallized samples were heated to 190°C, held for 5 min, cooled to 133°C at 10°C/min, and held at that temperature for 2.5 h. The samples were then quenched to room temperature and heated from 25 to 190°C at 10°C/min to observe the melting behavior.

Small samples were placed in a Mettler FP5 hot stage on a glass slide and heated to 190°C at 10°C/min and held for 5 min. After melting, a coverslide placed over the material was pressed down manually to produce a thin film, and then isothermal crystallization at 133°C was monitored for 2.5 h. Growth of the spherulites was observed in a transmission optical microscope under polarized light. Subsequently, some samples were cooled to room temperature and reheated at 1°C/min to observe the melting behavior.

Thin sheets (0.3 mm) of each compatibilizer were compression-molded from either pellets (LAC) or powder (HAC) at 2000 psi and 175°C for 5 min. Subsequently, each sheet was molded between two thicker PP sheets at 2000 psi and 175°C. Layer thicknesses were arranged so that one PP/compatibilizer interface lay at the midplane of the sample. A metal tab was used during molding to introduce a sharp notch on one edge. Thin strips of the trilayer samples (100 × 7 × 3.2 mm) were loaded in a double-cantilever beam configuration using a crosshead displacement speed of 5 mm/min.

RESULTS AND DISCUSSION

Melting and Crystallization

Initial DSC data were obtained with a heating/cooling rate of 10°C/min. Thermograms obtained on the second heating of the injection-molded PP control, the as-received HAC powder, and the as-received LAC pellets are compared in Figure 1. The DSC traces showed a melting point of 164.1°C for PP, which corresponded to previously reported values for PP.[6] The LAC exhibited a melting point of 160.4°C. The small peak evident at 117°C was due to the presence of polyethylene (PE) segments (7.8%), which was confirmed by NMR. The HAC exhibited a T_m of 154.6°C. The lower melting temperature of the compatibilizers was attributed to the lower molecular weight and to chain heterogeneity introduced by the anhydride groups. The drop in T_m, about 4°C for LAC and 10°C for HAC, paralleled both the decrease in molecular weight and the increased concentration of anhydride groups. In general, random substitution for hydrogens in polymer chains results in a reduction in T_m. Random branch substitution in PE can lower the T_m by more than 30°C as well as reduce the size and perfection of crystalline regions.[7] Random substitution of side chains of varying structure onto isotactic polypropylene is also known to decrease the melting temperature.[8–10] It is expected that anhydride grafted

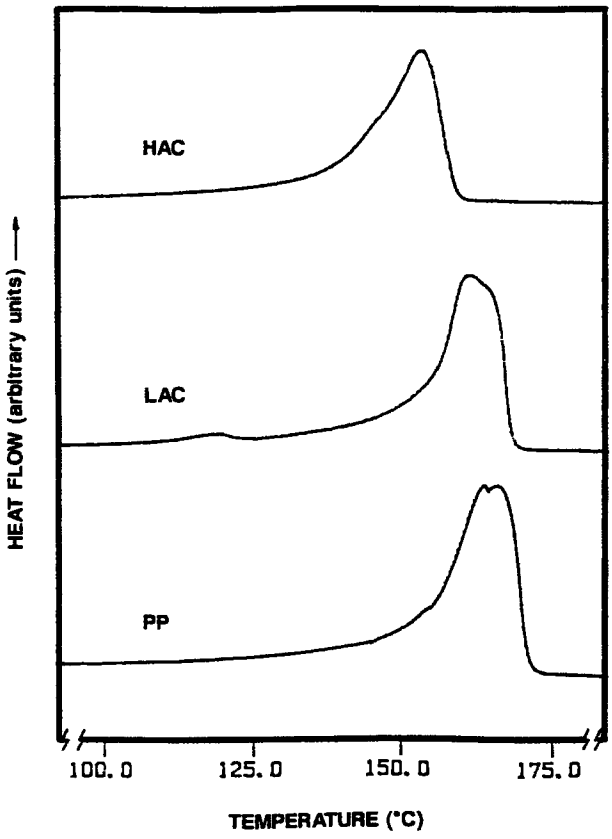

Figure 1 DSC thermograms taken at 10°/min. of HAC, LAC, and PP.

Table I Melting and Crystallization Data for PP, Compatibilizers, and Blends Obtained by DSC Using a Heating/Cooling Rate of 10°/Min

	T_m (°C) as Received	T_m (°C) Second Heating	% Cr[a] as Received	% Cr[a] Second Heating	T_c (°C)	$\Delta T_m - T_c$ (°C)
PP	165.8	164.1	45.5	50.0	115.7	48.4
LAC	163.9	160.4	35.5	38.1	118.5	41.9
HAC	155.3	154.6	44.8	36.0	109.1	45.5
PP/LAC 85/15	165.1	163.0	42.6	45.9	111.9	51.1
PP/HAC 85/15	165.5	162.2	44.2	47.7	113.0	49.2

[a] Based on total specimen weight and ΔH_f = 209 J/g for PP.[7]

onto the PP chain had a similar effect, which was magnified by increasing the number of anhydride groups. The differences in molecular weight also contributed to the decrease in T_m.[11]

Blending 15% of either compatibilizer with PP did not significantly affect the melting temperature or the total crystallinity when a heating/cooling rate of 10°C/min was used, as shown in Table I. The DSC endotherms were similar in shape, which suggested virtually no effect on melting of PP.

Isothermal Crystallization

Isothermal crystallization of PP and blends of PP with either compatibilizer were carried out in the DSC at 133°C, which represented an undercooling of $\Delta T = T_m - T_c$ = 33°C. This value was chosen to coincide with isothermal crystallization conditions used in previous studies.[12] As determined from subsequent heating thermograms, isothermal crystallization resulted in a slightly higher melting temperature but about the same level of crystallinity as crystallization during cooling at 10°C/min (Table II).

The heating thermograms of isothermally crystallized PP and PP blends with 15% compatibilizer are compared in Figure 2. The PP showed a sharp melting peak at 169°C with a broad tail on the low-temperature side beginning near the crystallization temperature of 133°C. The thermogram of PP with 15% LAC was indistinguishable from that of PP. However, the thermogram of the isothermally crystallized blend with 15% HAC revealed a second melting peak at 154°C in addition to the primary melting peak at 167°C. The temperature of the second melting endotherm in the blend with HAC coincided with the melting temperature of HAC. The appearance of a distinct melting peak attributable to the compatibilizer suggested that HAC, with an

Table II Isothermal Crystallization Data

	T_m (°C)	Crystallinity (%)
PP	169.0	51.1
PP/LAC (85/15)	166.9	46.3
PP/HAC (85/15)	166.9	48.1
	153.5	Sum of two peaks

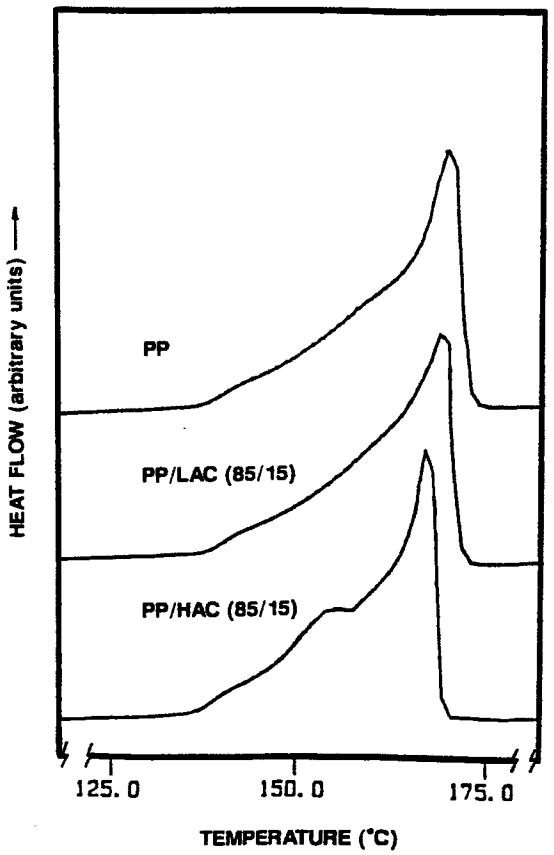

Figure 2 DSC thermograms of PP, PP/LAC (85/15), and PP/HAC (85/15) after isothermal crystallization at 133°C for 2.5 h.

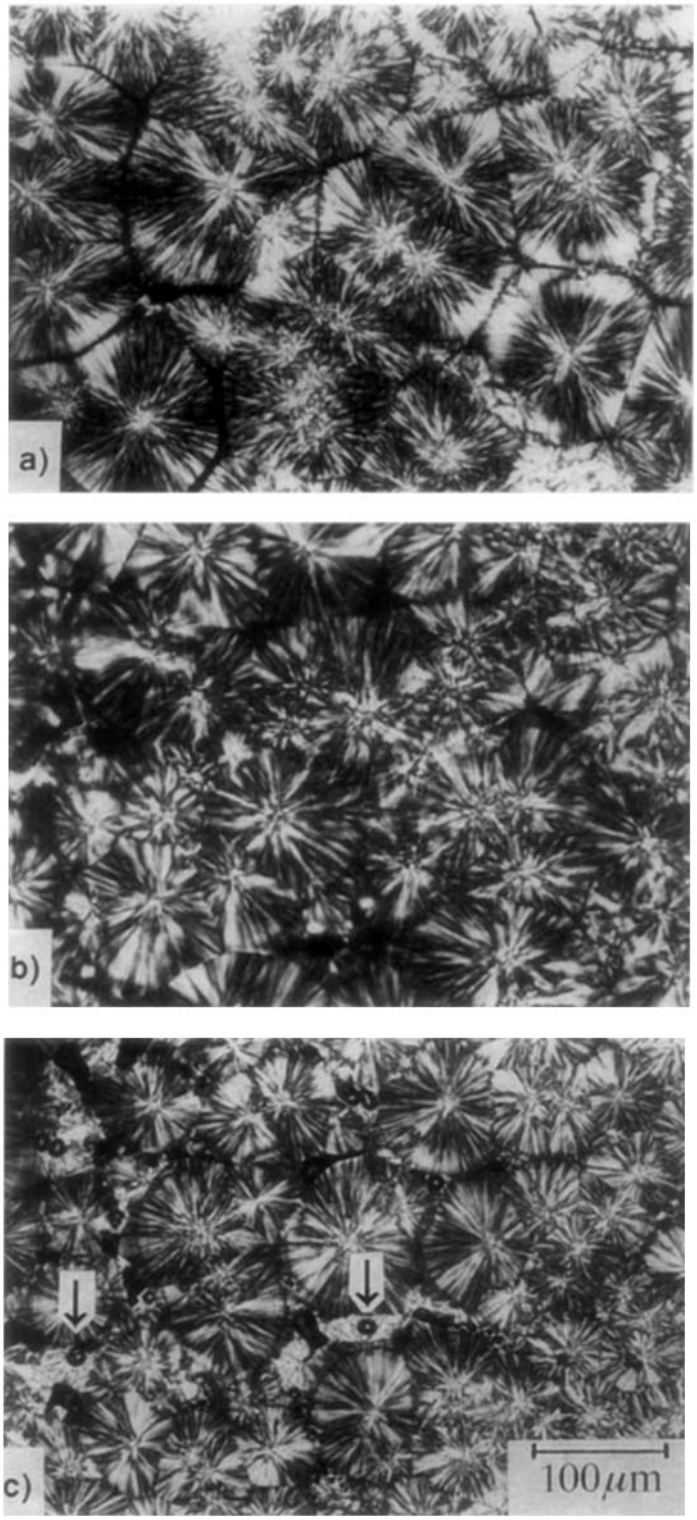

Figure 3 Optical micrographs showing (a) PP and (b) PP/LAC (85/15) with no interspherulitic material, and (c) PP/HAC (85/15), with randomly dispersed interspherulitic material indicated by the arrows.

average of six anhydride groups per chain and a lower molecular weight than that of LAC, crystallized as a separate phase.

The experimental conditions used in the isothermal crystallization experiment in the DSC were simulated on a hot stage in the optical microscope. Figure 3 shows the morphology of thin films isothermally crystallized from the melt. The spherulites in the PP specimen shown in Figure 3(a) had an average diameter of 90 μm and displayed the characteristic birefringence of type I spherulites described in the literature.[6,13] Spherulites in the PP/LAC (85/15) blend shown in Figure 3(b) also had an average spherulite size around 90 μm, but exhibited a slightly different birefringence from PP. The absence of interspherulitic material in this blend suggested that LAC cocrystallized with PP and, moreover, that the LAC altered the spherulite structure sufficiently to produce a change in birefringence. The average spherulite diameter in the blend with 15% HAC [Fig. 3(c)] was 70 μm, slightly smaller than that of PP or the LAC blend. In this case, crystallizable interspherulitic material was observed. The birefringence patterns indicated that the material dispersed between the spherulites crystallized with a much finer texture than that of the PP. A sequence of photographs in Figure 4 shows the isothermal crystallization at 133°C of PP blended with 15% HAC. After 56 min, when the type I PP spherulites were fully developed, a black uncrystallized area remained [box in Fig. 5(a)]. Subsequently, at about 60 min, spherulites that exhibited a different birefringence started to grow in the black area. Crystallization of the second phase continued slowly until eventually it filled the area.

After 2.5 h at 133°C, the same specimen was quenched to ambient temperature and the sequence of photographs in Figure 5 was obtained as the sample was subsequently heated at 1°C/min. Between 154 and 155°C, the spherulites in the second phase melted completely while the regular polypropylene spherulites remained unchanged. The melting temperature of the second phase matched the T_m of HAC. This visually confirmed the conclusion drawn from the DSC thermograms of isothermally crystallized blends, specifically that HAC did not cocrystallize with PP but crystallized independently as a separate phase. It was highly unlikely that the separated material was an ungrafted, low molecular weight fraction of HAC. Analysis of the compatibilizers given previously indicated that HAC consisted of uniformly grafted chains. Furthermore, the area occupied by this phase was approximately 15%, which was the weight fraction of HAC in the blend.

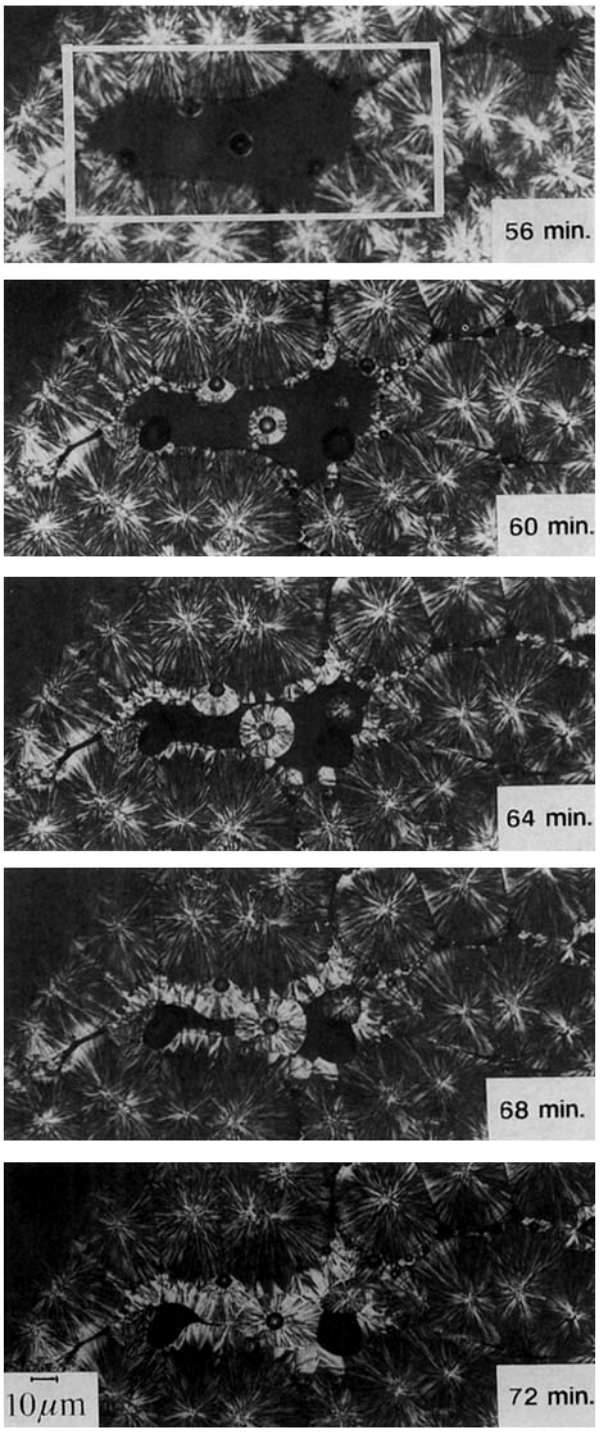

Figure 4 Sequence of photographs during isothermal crystallization of PP/HAC (85/15) at 133°C.

Cocrystallization and Phase Separation Models

One function of the compatibilizer is to promote interfacial adhesion and enhance stress transfer between phases in the solid state. In principle, adhe-

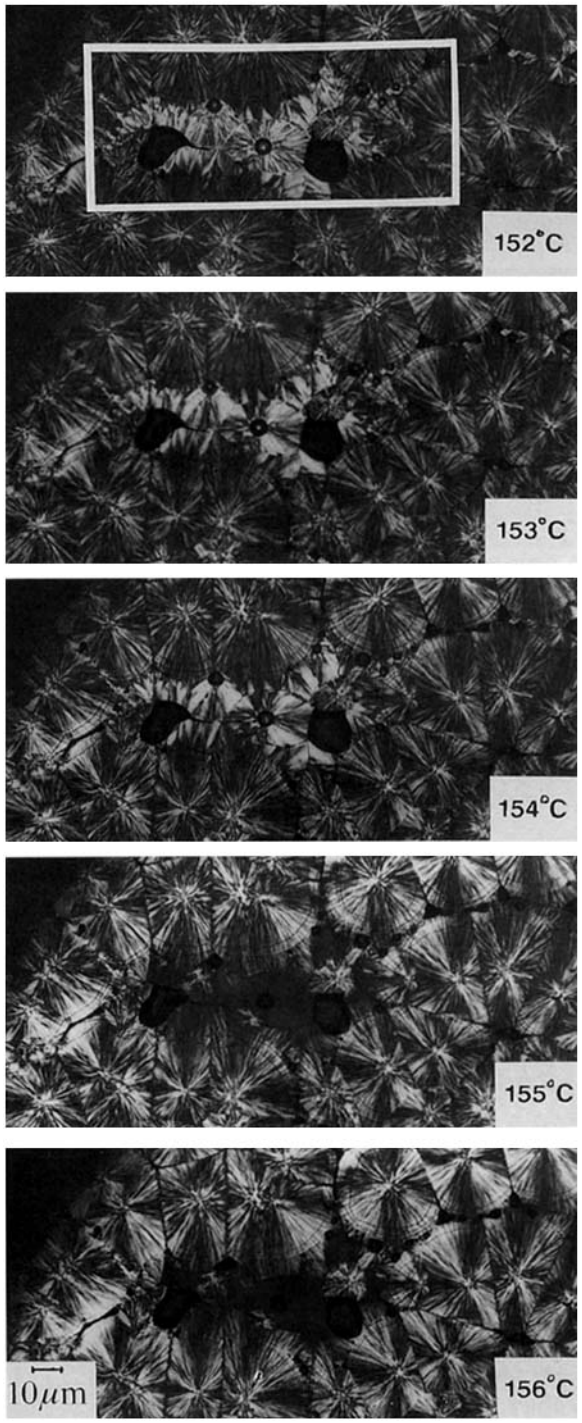

Figure 5 Sequence of photographs during subsequent melting of the PP/HAC (85/15) sample in Figure 4.

sion in PP/PA blends is achieved with PP-*g*-MA compatibilizers by chemical reaction with the PA, while relying on the chemical similarity of PP and the grafted PP for adhesion to the PP phase. Based on this generally accepted concept of compatibilization of PP/PA blends, it can be anticipated that the degree to which satisfactory interfacial adhesion is achieved will be influenced by the affinity of the PP-*g*-MA compatibilizer for the PP phase.

The apparent cocrystallization of PP with LAC compared to phase-separated crystallization of HAC led to the proposal of two interfacial models for compatibilized PP/PA blends. A cocrystallization model for LAC is shown schematically in Figure 6. Most of the maleic anhydride groups in this compatibilizer are on the chain ends. The model shows the compatibilizer molecules (shaded molecules) chemically linked to the PA phase as a result of reaction between the maleic anhydride and terminal anhydride groups of the PA during processing. The model also indicates that the concentration of maleic anhydride groups is sufficiently low (one per chain on average) and the molecular weight high enough (135,000) that the LAC molecules cocrystallize with PP (white molecules) during subsequent solidification. The compatibilizer promotes an interphase region with good adhesion where adherence to the PP phase is achieved by cocrystallization and to the PA phase by chemical linkages.

A separate phase model for compatibilization of PP/PA blends with HAC is shown schematically in Figure 7. With an average of six anhydride groups per chain, only some of the anhydride groups of HAC (shaded molecules) are shown to be chemically reacted with the PA. The low molecular weight (52,000) and high concentration of chain substitution of HAC favor crystallization of HAC as a separate phase from PP (white molecules). The HAC promotes an interphase with more chemical linkages to the PA phase than that of LAC, but with less effective coupling to the PP phase.

Adhesion Measurements

The double cantilever beam (peel) method[14-16] was used to test the proposed models by comparing the physical adhesion between PP and each compatibilizer. Trilayer samples consisting of two outer PP layers and a center layer of LAC or HAC were used to determine the adhesion between PP and compatibilizer. Figure 8 shows the load-displacement curves for propagation of a crack through the PP/compatibilizer interface of PP/LAC/PP and PP/HAC/PP samples. The higher load required to propagate a crack in PP/LAC/PP indicated stronger adhesion between PP and LAC than between PP and HAC. The irregular, saw-tooth shape of the PP/LAC/PP load-displacement curve was characteristic of discontinuous crack growth. The stop–

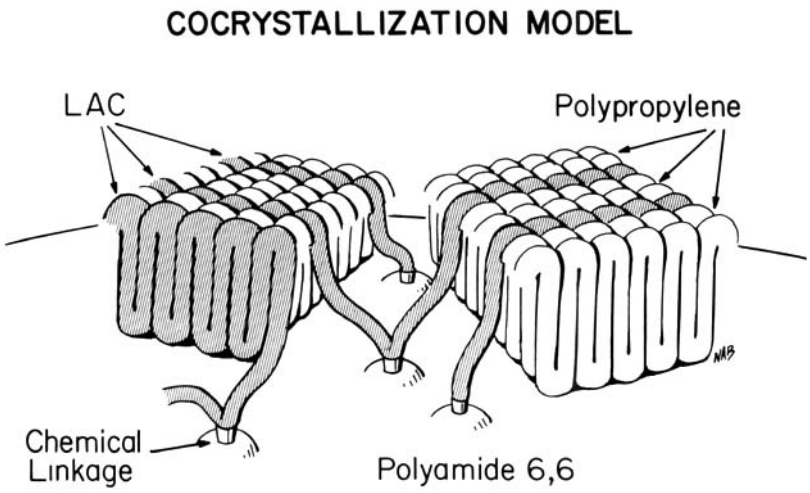

Figure 6 Schematic representation of cocrystallization of PP and LAC near the PA particle surface with anhydride groups on LAC chemically reacted with PA and free chain ends cocrystallized with surrounding PP.

start propagation was apparent visually when the crack was observed to arrest at a load minimum; the bend angles would then gradually increase with a gradually increasing load until the crack jumped forward as the load dropped sharply. About 70% of the fracture surface of PP/LAC/PP was stress-whitened, indicative of cohesive failure with plastic deformation. Sometimes the maxima in the load displacement curve correlated with regions of intense stress-whitening. This was the case, e.g., with the large load peak at about 100 mm displacement. Other load peaks, however, did not directly correspond with features on the fracture surface.

In contrast, the load-displacement curve of PP/HAC/PP was relatively flat, indicative of continuous crack propagation. This was confirmed by visual observation of crack growth in PP/HAC/PP. Only about 10% of the fracture surface was stress-whitened. Failure was assumed to be adhesive in regions where there was no stress-whitening.

The bend angles measured at intervals during the peel tests are shown in Figure 9. Much higher bend

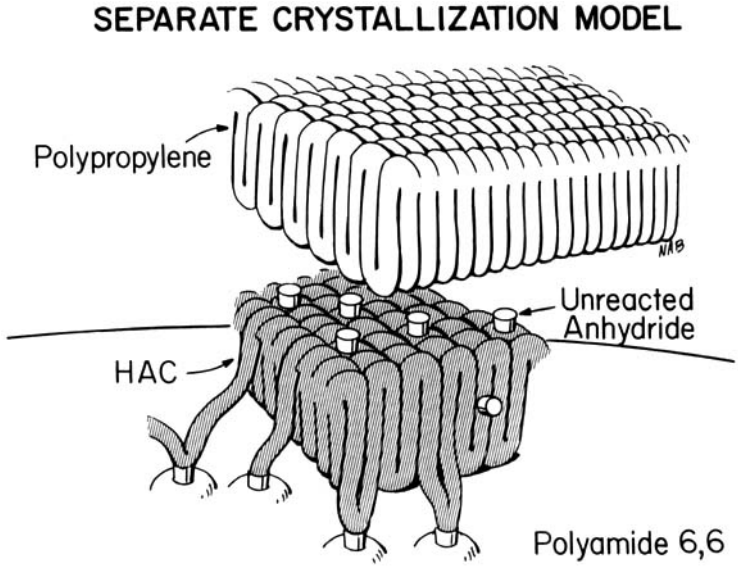

Figure 7 Schematic representation of separate phase crystallization of PP and HAC near the PA particle surface, with high concentration of reacted and unreacted anhydride groups on HAC causing segregation of HAC from PP.

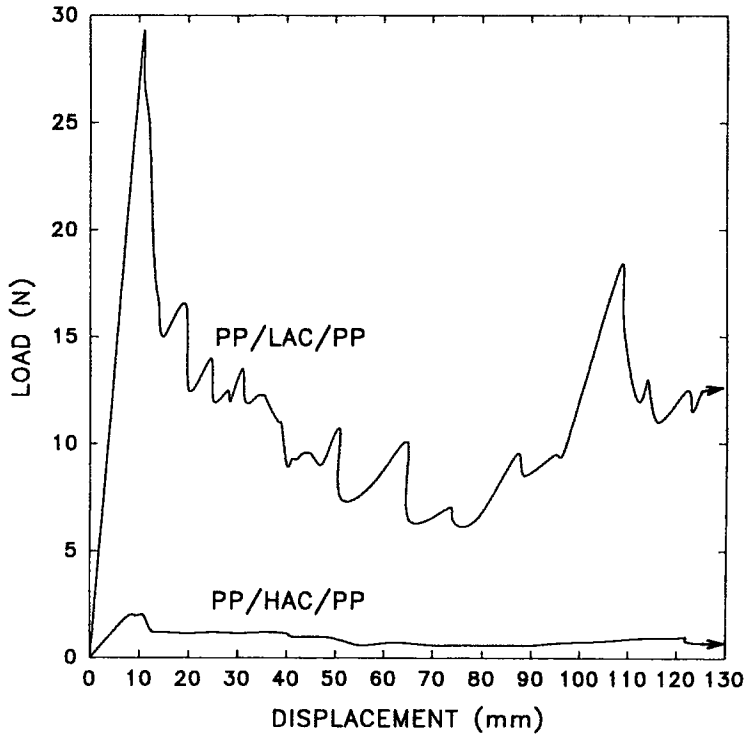

Figure 8 Load-displacement curves for PP/LAC/PP and PP/HAC/PP samples.

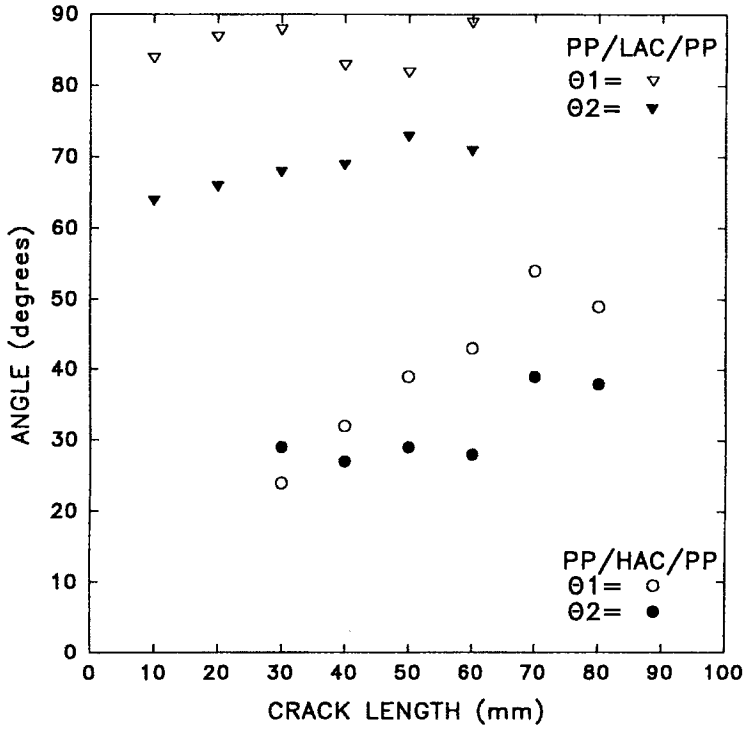

Figure 9 The bend angles measured at several intervals during the peel tests. Points for PP/LAC/PP were taken at peak stresses in the load-displacement curve.

angles were observed with PP/LAC/PP, consistent with the higher loads required to propagate a crack. While the test approached a T-peel test with $\Theta_1 = \Theta_2 = 90°$ for PP/LAC/PP, the angles were considerably less than 90° for PP/HAC/PP. Furthermore, the angles were not constant, but increased gradually during the test. When the angles are not 90°, the mode I fracture toughness, G_{IC} can be calculated by

$$G_{IC} = \frac{P_C(\sin \Theta_1 + \sin \Theta_2)}{w} \quad (1)$$

where P_C is the critical load; Θ_1 and Θ_2, the bend angles; and w, the sample width. The fracture toughness calculated at several points during the test is plotted in Figure 10. The values for PP/HAC/PP were relatively constant at about 190 ± 20 J/m^2, which was consistent with continuous crack growth. The values for PP/LAC/PP were much higher, in the range of 3200 ± 385 J/m^2, and were more variable. Critical loads in this case were taken at peaks in the load displacement curve where the crack jumped. The large range in G_{IC} reflected variability in the amount of plastic deformation that accumulated during crack arrest.

Good adhesion of LAC to PP was apparent from the high fracture toughness that accompanied predominantly cohesive failure with plastic deformation. This compared with much lower fracture toughness and predominantly adhesive failure between HAC and PP. It was concluded that during compression molding intimate contact in the melt state allowed the interdiffusion and subsequent cocrystallization of PP and LAC. Under the same conditions, it appeared that PP and HAC did not interdiffuse.

A manifestation of this difference was found in the higher fracture strains of PP blends with 25% PA compatibilized with LAC compared to the same blends compatibilized with HAC. In the interfacial region between the two phases, cocrystallization of LAC with the PP phase, combined with the chemical linkage of LAC to the PA dispersed phase, resulted in adhesion that was strong enough to prevent interfacial failure as the PP was drawn out. Since the PA particles remained enmeshed in the drawn PP network, they were not sites of voiding and crack initiation. HAC also provided chemical linkage to the PA dispersed phase; however, the phase segregation of HAC and PP near the interface resulted in an adhesion strength that appeared to be lower than the draw stress of PP. Therefore, interfacial failure occurred as the PP matrix began to draw,

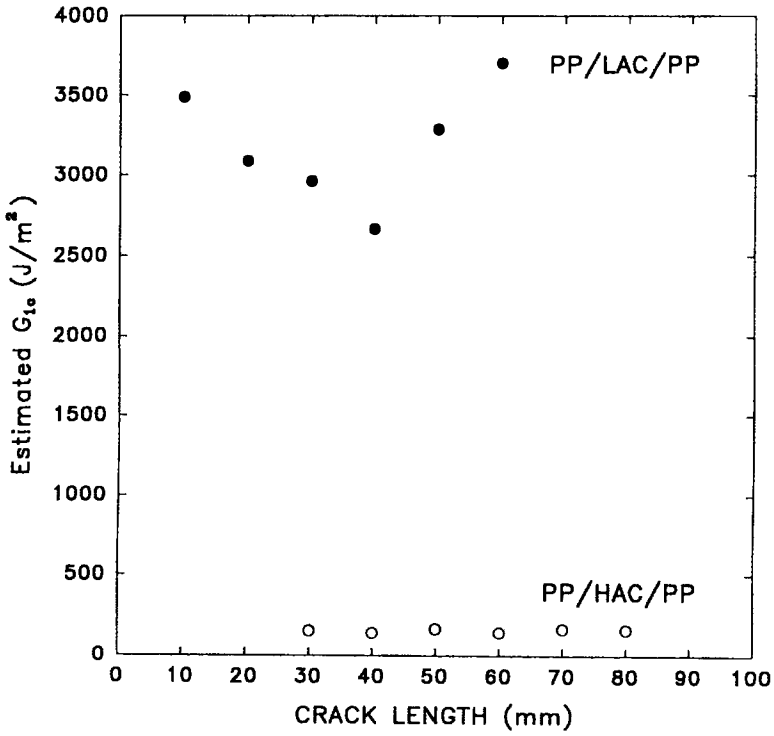

Figure 10 Estimated fracture toughness (G_{IC}) of PP/LAC/PP and PP/HAC/PP. Points for PP/LAC/PP were taken at peak stresses in the load-displacement curve.

which produced voids and eventually sites for crack initiation.

CONCLUSIONS

The LAC appears to cocrystallize with PP as PP/LAC blends exhibit one melting peak and a single spherulite type is observed by optical microscopy. Cocrystallization is possible due to low grafted maleic anhydride and relatively high molecular weight of LAC. A cocrystallization model is proposed for PP-rich PP/PA blends compatibilized with LAC, which predicts good adhesion due to concurrent chemical linkage to dispersed PA and cocrystallization with the PP matrix.

The HAC phase separates from PP as seen by separate melting peaks in PP/HAC blends for each component and observation in the optical microscope of a second crystalline form which melts at the T_m of HAC. Phase separation occurs due to a high amount of grafted maleic anhydride and a low molecular weight of HAC. A separate phase crystallization model is proposed for PP-rich PP/PA blends compatibilized with HAC, which predicts poorer adhesion due to phase segregation of PP and the HAC segments of HAC-*g*-PA near the PA particle surfaces. Peel tests established the correlation between blend mechanical properties and the crystallization models when a 10-fold higher adhesion strength was measured between PP and LAC compared to PP and HAC.

The authors thank the Amoco Chemical Co. for financial support of this work and for supplying the materials. The Amoco Corporate Research Laboratory provided FTIR, NMR, and titration analyses. Polymer blend extrusion, molding, and purification of analytical samples were performed by members of the Polymer Applications Group, especially by M. Wreschinsky.

REFERENCES

1. F. Ide and A. Hasegawa, *J. Appl. Polym. Sci.*, **18,** 963 (1974).
2. S. Hosoda, K. Kojima, Y. Kanda, and M. Aoyagi, *Polym. Networks Blends,* **1,** 51 (1991).
3. S. J. Park, B. K. Kim, and H. M. Jeong, *Eur. Polym. J.*, **26,** 131 (1990).
4. R. Holsti-Miettinen, J. Seppala, and O. T. Ikkala, *Polym. Eng. Sci.*, **32,** 868 (1992).
5. J. Duvall, C. Sellitti, C. Myers, A. Hiltner, and E. Baer, **52,** 195 (1994).
6. F. J. Padden, Jr. and H. D. Keith, *J. Appl. Phys.*, **30,** 1479 (1959).
7. J. Brandup and E. H. Immergut, *Polymer Handbook,* 3rd ed., Wiley-Interscience, NY, 1989, V15–V28.
8. F. W. Billmeyer, *Textbook of Polymer Science,* 3rd ed., Wiley-Interscience, New York, 1984, Chap. 12, pp. 331–335.
9. T. W. Campbell and A. C. Haven, Jr., *J. Appl. Polym. Sci.*, **1,** 73 (1959).
10. C. E. H. Bawn, *Chem. Ind.*, 388 (1960).
11. M. J. Hill, P. J. Barham, and A. Keller, *Polymer,* **33,** 2530 (1992).
12. C. J. Chou, K. Vijayan, D. Kirby, A. Hiltner, E. Baer, *J. Mater. Sci.*, **23,** 2521 (1988).
13. F. J. Padden Jr. and H. D. Keith, *J. Appl. Phys.*, **30,** 1485 (1959).
14. S. Wu, *Polymer Interface and Adhesion,* Marcel Dekker, New York, 1983.
15. D. Satas, *Handbook of Pressure Sensitive Adhesive Technology,* Van Nostrand Reinhold, New York, 1982.
16. J. G. Williams, *J. Comp. Mater.*, **21,** 330 (1987).

Received September 24, 1993
Accepted October 5, 1993